Grid Phase Synchronization via Distributed Control

Andrei Sperilă
Laboratoire des Signaux et Systèmes
CentraleSupélec, Paris-Saclay University
Gif-sur-Yvette, France
andrei.sperila@centralesupelec.fr

Alessio Iovine
Laboratoire des Signaux et Systèmes
CentraleSupélec, Paris-Saclay University
Gif-sur-Yvette, France
alessio.iovine@centralesupelec.fr

Sorin Olaru
Laboratoire des Signaux et Systèmes
CentraleSupélec, Paris-Saclay University
Gif-sur-Yvette, France
sorin.olaru@centralesupelec.fr

Patrick Panciatici
Laboratoire des Signaux et Systèmes
CentraleSupélec, Paris-Saclay University
Gif-sur-Yvette, France
patrick.panciatici@ieee.org

***Abstract*—The problem of synchronizing the electrical angles of a power system's nodes is investigated in the distributed setting, in which only partial grid information is available at each of the aforementioned nodes. The proposed control solution takes the form of a novel two-layer regulatory architecture. The first layer ensures the stabilization of the grid's dynamics and the dynamical decoupling of its nodes, with respect to exogenous disturbance. The second layer employs predictive control strategies in order to ensure phase synchronization, while also enforcing limits on power injections. The computational cost of the proposed solution boils down to implementing a recurrence equation and to solving a linear optimization problem, at each of the grid's nodes.**

***Index Terms*—Power grids, phase synchronization, distributed control, linear programming, scalable implementations**

I. Introduction

A. Context and Motivation

The growing complexity of modern power systems represents the chief obstacle in the way of ensuring safe and efficient energy transmission. As national power grids become more and more interconnected with their European (indeed, even intercontinental) counterparts, locally designed and implemented control strategies have noticeably struggled to keep up with the ever-increasing demands placed upon them [1]. An especially important problem that needs to be addressed in such emerging configurations is that of synchronizing the grid's nodes, with respect to their parameters [2]–[4]. Due to the widely dispersed nature of the aforementioned grids, the node-based control laws which ensure this synchronization must often operate using partial grid information, gathered from a neighbourhood of their assigned node. While several distributed control solutions [5]–[8] are able to tackle this challenge, their theoretically involved formulations and possibly high computational costs detract from their applicability.

The main problem discussed in this paper is that of synchronizing all the electrical angles of a power grid's nodes to a single reference signal, in the presence of communication constraints between the aforementioned nodes. In addition to this, the secondary objectives of limiting power injection and attenuating the effects of exogenous disturbance upon the nodes' electrical angles are also addressed, in tandem with the distributed synchronization problem. In order to simultaneously achieve all of these aims, we propose a novel type of control architecture, based upon a combination of two powerful and modern techniques:

- $i)$ the distributed control laws based upon the Network Realization Function (NRF) representation, prototyped in [9] and theoretically formalized in [10] and [11];
- $ii)$ the class of Model Predictive Control (MPC) strategies whose optimization-based formulations (see, for example, [12] and [13]) have recently gained a notable amount of traction in the industrial setting.

In the sequel, we show how these two control techniques can be elegantly blended into a practical design framework, and how the latter generates a class of control laws that are capable of successfully tackling the grid synchronization problem in the distributed setting.

B. Contributions

Our chief contribution lies in providing a highly practical and easy to implement control scheme, which is able to handle the threefold objective of: phase synchronization, power injection limitation, and disturbance attenuation. Not only do we provide a hands-on and implementation-centric perspective on the grid synchronization problem, but we also achieve all of these objectives in a purely distributed setting, in which multiple subcontrollers exchange information and undertake concerted efforts to ensure safe and efficient plant operation.

Finally, we illustrate a concrete example of the design framework discussed in this paper, in which we show how to implement our two-layer control scheme for a grid synchronization application, based upon the swing dynamics discussed in [14]. The latter are particularly well suited for describing the behaviour of power transmission systems (see [14], along with the references therein), and it constitutes a benchmark for numerous problems in distributed control literature [6]–[8].

C. Paper Structure

In Section II, we describe the dynamics and the topology of the power grid, while also laying out the objectives which have to be achieved by our regulatory solution. In Section III, we first introduce the NRF-based control laws, and we then state the formulations of the optimization problems which designate our MPC-based subcontrollers. In Section IV, we present the parameters and the explicit forms of the grid's control laws. Moreover, we showcase a simple yet illustrative simulation scenario, which highlights the benefits of the proposed solution. Finally, Section V offers a set of concluding remarks.

II. Grid Dynamics and Control Objectives

A. The Network Model

The grid takes the form of a mesh, whose nodes are governed by the linearized swing dynamics of the type discussed in [14] and discretized as in [6]–[8], given explicitly by

$$x_i[k+1] = \sum_{j=1}^{N} A_{ij} x_j[k] + B_i(u_i[k] + w_i[k]), \quad (1)$$

where we have that:

a) the i^{th} node's state vector $x_i[k] = \begin{bmatrix}\delta_i[k] & \omega_i[k]\end{bmatrix}^\top$ is composed of the node's rated electrical frequency $\omega_i[k]$, *i.e.*, the value that has been centred around and normalized by 2π times the grid's nominal frequency, and of the corresponding electrical angle $\delta_i[k]$;

b) the controllable power injection of the i^{th} node, which enables actuation, is denoted by $u_i[k]$;

c) the i^{th} node's input disturbance injection is $w_i[k]$;

d) the discretization step of the swing dynamics is equal to $\Delta t = 0.2$ s;

e) the coefficient matrices A_{ij} and B_i are expressed, for all $i \in \{1:N\}$, as follows

$$A_{ij} := \begin{cases} \begin{bmatrix} 1 & \Delta t \\ -h_i \Delta t \sum_{q=1}^{N} \ell_{iq} & 1 - h_i d_i \Delta t \end{bmatrix}, \ i = j, \\ \begin{bmatrix} 0 & 0 \\ h_i \ell_{ij} \Delta t & 0 \end{bmatrix}, \ i \neq j, \end{cases} \quad (2a)$$

$$B_i := \begin{bmatrix} 0 & 1 \end{bmatrix}^\top; \quad (2b)$$

f) the physical parameters appearing in (2a), namely: h_i (inverse of the rotational inertia), d_i (damping factor) and ℓ_{ij} (coupling factor) are uniformly distributed within the intervals $[0.2, 2]$, $[0.5, 1]$ and $[0.5, 1]$, respectively.

We assume that each node is equipped with a controllable injection unit (allowing for $u_i[k]$), with a phase measurement unit, and with a frequency sensor. Therefore, $x_i[k]$ is *locally* available for measurement and the possibility of transmitting it to other nodes' subcontrollers will be carefully discussed in the sequel. In addition to this, we consider (for the simulations presented in this paper) a network described by $N = 5$ nodes and by the numerical values given in Table I, located on the right-hand column of this page. Upon inspecting the numerical data displayed in the aforementioned table, it is straightforward

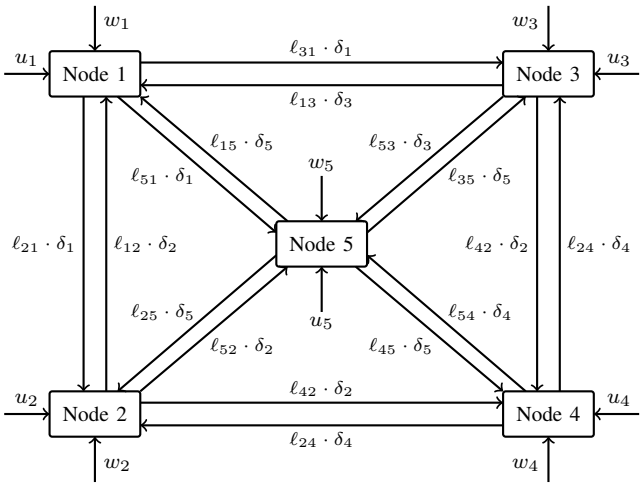

Fig. 1. Interconnection topology of the power grid's dynamics

i	h_i	d_i	ℓ_{i1}	ℓ_{i2}	ℓ_{i3}	ℓ_{i4}	ℓ_{i5}
1	0.3244	0.5650	0	0.6511	0.7915	0	0.7513
2	1.5886	0.7844	0.6511	0	0	0.8433	0.6318
3	0.6224	0.7347	0.7915	0	0	0.8259	0.8620
4	1.0571	0.5060	0	0.8433	0.8259	0	0.8367
5	0.3313	0.6686	0.7513	0.6318	0.8620	0.8367	0

TABLE I
Values of the parameters appearing in (2a)

to check that the matrices A_{ii} have eigenvalues only inside the unit circle, for all $i \in \{1:N\}$. Thus, it follows that the *local* phase oscillation dynamics are stable. However, by inspecting the *global* dynamics of the grid, whose state vector is given by $x[k] = \begin{bmatrix} x_1^\top[k] & x_2^\top[k] & x_3^\top[k] & x_4^\top[k] & x_5^\top[k] \end{bmatrix}^\top$, we point out that the resulting state matrix has an eigenvalue in $z = 1$.

Remark II.1. *One of the main design challenges associated with networked system control is the fact that, even if all of the grid's components possess stable dynamics, their interconnection often leads to networks with unstable behaviour. Therefore, the need to obtain stabilizing (and distributed) control laws is a very real concern in most practical applications.*

B. The Topology of the Grid

Aside from stability, the network's topology is yet another factor which plays a key role in the design of (distributed) control laws. As indicated by the integer N, our network is partitioned into five separate nodes, whose dynamics are given by (1). The state-based cross-coupling appearing in (1) directly determines the interconnection topology of the network, which is displayed graphically in Figure 1, located at the top of this column. In accordance with the interconnections showcased in this figure, we denote the adjacency matrix of the network's directed graph representation via the following binary matrix

$$L = \begin{bmatrix} 0 & 1 & 1 & 0 & 1 \\ 1 & 0 & 0 & 1 & 1 \\ 1 & 0 & 0 & 1 & 1 \\ 0 & 1 & 1 & 0 & 1 \\ 1 & 1 & 1 & 1 & 0 \end{bmatrix},$$

where each entry L_{ij} is equal to the truth value of $\ell_{ij} \neq 0$.

The final critical factor which impacts the design of the control laws presented in this paper is the communication infrastructure of the network. The latter is represented by a set of neighbourhoods $\mathcal{N}_i \subseteq \{1:N\}$, $\forall\, i \in \{1:N\}$, in which $\mathcal{N}_i$ designates (by collecting their indices) the nodes which are able to transmit their state and controlled input information to the i^{th} node. For the benchmark depicted in Figure 1, we have

$$\begin{aligned} \mathcal{N}_1 = \{1,2,3,5\},\ \mathcal{N}_2 = \{1,2,4,5\},\ \mathcal{N}_3 = \{1,3,4,5\}, \\ \mathcal{N}_4 = \{2,3,4,5\},\ \mathcal{N}_5 = \{1,2,3,4,5\}. \end{aligned} \tag{3}$$

Having clarified both the dynamics and the topology of our power system, we now present a series of objectives which must be achieved by the grid's companion control system, in order to guarantee the network's safe and efficient functioning.

C. Design Specifications

In order to highlight the distributed nature of our proposed solution, we proceed to formulate our design objectives with respect to the local control laws of an arbitrarily chosen i^{th} node. This local subcontroller must:

- $i)$ employ information only from $\mathcal{N}_i$ to compute $u_i[k]$;
- $ii)$ coordinate its efforts with all other subcontrollers, in order to stabilize the global dynamics of the grid;
- $iii)$ dynamically decouple $x_i[k]$ from all $w_j[k]$, with $j \neq i$;
- $iv)$ ensure that $\delta_i[k]$ tracks a prescribed reference $r[k]$;
- $v)$ satisfy the constraint $|u_i[k]| \leq u_{\text{lim}}$.

We point out that our five objectives separate naturally into two categories. The ones from points $i)$–$iii)$ can be elegantly handled by the distributed control technique developed in [10], [11] and, by exploiting the satisfaction of point $iii)$, individual MPC controllers can then be designed for each of the grid's nodes, in order to tackle the objectives stated in points $iv)$–$v)$.

Remark II.2. *Notice that the reference signal $r[k]$, appearing in point $iv)$ above, is the same for every node. This comes as no surprise, given that the goal of this paper is to synchronize the electrical angles of all the grid's nodes. We point out, however, that the focus of our work rests solely with ensuring the tracking of this signal. Thus, we do not concern ourselves with its computation and propagation throughout the network, and we assume that $r[k]$ is made accessible at each node (through various pre-computation and node-hopping strategies).*

With the mathematical model of the network now clarified, and its associated objectives clearly stated, we now present the twin control algorithms which make up our regulation scheme.

III. The Distributed Control Solution

As discussed in Section II-C, the control system presented in this paper is made up of two separate, but coordinated, components. We denote by $u_{1i}[k]$ the control action computed by the i^{th} node's NRF-based subcontroller, and by $u_{2i}[k]$ the command signals produced by the i^{th} node's MPC-based subcontroller. Thus, for each $i \in \{1:N\}$, the total control action of a node will be computed as $u_i[k] = u_{1i}[k] + u_{2i}[k]$, and we begin our discussion with the computation of $u_{1i}[k]$.

A. NRF-based Stabilization and Decoupling

The first hurdle which needs to be overcome by our proposed control scheme is the stabilization of the grid's dynamics (recall Remark II.1). Notably, the class of all stabilizing controllers for a linear and time invariant system, such as the one given in (1), takes the form of the celebrated Youla Parametrization (see, for example, Chapter 12 in [15]). In order to overcome the centralized nature of this parametrization, the work presented in [10] proposed an adaptation of the Youla-based design framework, which resulted in the formalization of a new class of distributed and stabilizing controllers.

With the aim of providing a more intuitive perspective on the NRF-based controllers introduced in [10], we present their formulations in a recurrence equation form. The most striking feature of these control laws is their distinctive feedback-feedforward structure, in which the control laws (particularized for the model discussed in Section II) take the form

$$u_{1i}[k] = \sum_{j \in \mathcal{N}_i} \sum_{q=1}^{\tau_i} \left(\phi_{ijq} u_{1j}[k-q] + \gamma_{ijq}^{\top} x_j[k-q] \right), \tag{4}$$

where we have that:

a) the scalars $\phi_{ijq} \in \mathbb{R}$ and the vectors $\gamma_{ijq} \in \mathbb{R}^2$ represent the coefficients of the recursive equation given in (4);

b) the non-zero integers τ_i represent the maximum amount of previously memorized command and state-feedback values employed to compute[1] $u_{1i}[k]$.

Remark III.1. *The sparsity-promoting procedure from [11] translates into a model-matching problem which adjusts the coefficients encoded in ϕ_{ijq} and in γ_{ijq}. By cancelling the latter out, the strain on the communication infrastructure of the network is reduced, while also desensitizing $u_{1i}[k]$ to measurement and communication noise, especially for those nodes which transmit particularly noise-affected information.*

In addition to the classical state-feedback $\gamma_{ijq}^{\top} x_j[k-q]$, the control laws from (4) also contain the feedforward terms $\phi_{ijq} u_{1j}[k-q]$, and we point out that including the latter is a popular choice when implementing grid synchronization strategies (see [16]). From a practical perspective, these terms play an important role in attenuating the propagation of disturbance through a network of interconnected systems, which is done by incorporating the control actions of neighbouring nodes into the decision process (see also the vehicle platooning application in [9], for an example of the benefits associated with this feedforward strategy). In order to achieve this attenuation, while also stabilizing the grid's dynamics, we present an implementation-centric design algorithm for the control laws stated in (4). This procedure is structured as follows:

- $i)$ use the state-space dynamics in (1) to form the factorizations given in Theorem II.1 of [11];
- $ii)$ use these factors to form the $\mathbf{Q}$-parametrized expressions given in Theorem II.6 of [10], for all closed-loop maps from $w_j[k]$ to $x_i[k]$ with $i \neq j$;

[1]For implementation purposes, queue-like memory buffers can be used to store the consecutive values of $u_{1j}[k]$ and $x_j[k]$ employed in (4). The maximum length of any such memory buffer for the i^{th} node is precisely τ_i.

$$\delta_i[k+2] = \begin{bmatrix} 1 & 0 \end{bmatrix} A_{ii} x_i[k+1] = \begin{bmatrix} 1 & 0 \end{bmatrix} A_{ii}(A_{ii}x_i[k] + B_i(u_i[k] + w_i[k])) + h_i(\Delta t)^2 \sum_{j \neq i} \ell_{ij}\delta_j[k]. \tag{6}$$

iii) use the model-matching procedures given in Sections III and IV of [11] to minimize the $\mathcal{H}_\infty$ system norm (see also [17], for a related approach in grid synchronization) of the aforementioned maps, for a *stable* $\mathbf{Q}$-parameter;

iv) use the obtained $\mathbf{Q}$-parameter to form the expressions from Section III of [10], and convert the state-space-based NRF subcontrollers to the form given in (4).

B. MPC-based Tracking and Command Limitation

The second part of our control solution consists in designing an MPC-based subcontroller for each of the grid's nodes. We propose a simple Linear Programming-based approach in which, for every $i \in \{1 : N\}$, we compute an additional control signal that adapts the NRF-based command in order to achieve the objectives from points *iv*) and *v*) in Section II-C.

Before going into further details, we point out that we are able to compute $u_{2i}[k]$ in the described manner only due to the control action provided by the NRF-based subcontrollers. Indeed, since objective *iii*) is successfully handled by the control laws discussed in Section III-A, and since $u_{2j}[k]$ can be assimilated with $w_j[k]$ (from the perspective of NRF-controlled closed-loop system), it follows that the commands computed by the j^{th} node's MPC-based subcontrollers will have a negligible impact upon $x_i[k]$, for all $j \neq i$. Thus, we may design each node's MPC-based subcontroller without having to concern ourselves with significant cross-coupling induced by control action of the other nodes' MPC policies.

The optimization problem which designates the i^{th} node's MPC-based subcontroller possesses a linear programming-based formulation, which is given explicitly by

$$\begin{aligned} &\min_{u_{2i}[k]} \ \beta_{ui}\varepsilon_{ui} + \beta_{ri}\varepsilon_{ri} \\ &\text{subject to} \begin{cases} 0 \leq \varepsilon_{ri}, \ 0 \leq \varepsilon_{ui} \leq u_{\text{lim}}, \\ |u_{1i}[k] + u_{2i}[k]| \leq \varepsilon_{ui}, \\ \left| r[k+2] - \widehat{\delta}_i[k+2|k] \right| \leq \varepsilon_{ri}, \end{cases} \end{aligned} \tag{5}$$

where we have that:

a) the slack variables ε_{ui} and ε_{ri} are employed as upper bounds on the absolute values of the power injection and of the electrical angle tracking error, respectively;

b) the scalars $\beta_{ui} > 0$ and $\beta_{ri} > 0$ are the constant weights[2] of the slack variables described in point a);

c) the variable $\widehat{\delta}_i[k+2|k]$ is the *two-step predicted value* of the i^{th} node's electrical angle, which is computed *locally* at the current time step.

It is straightforward to notice that the problem stated in (5) is exceptionally inexpensive to solve, from a computational standpoint, and that (in contrast to other, more theoretically-involved formulations) it poses no problems from the point of view of its feasibility. The only challenge, therefore, rests with obtaining reliable predictions for $\delta_i[k+2]$ without using any information from outside of $\mathcal{N}_i$. The crucial observation which renders this prediction reliable is obtained by first writing out the identity from (6), which is located at the top of this page. Since the electrical angles of all other nodes in the grid are weighted by $(\Delta t)^2$ in the aforementioned expression, it follows that $\widehat{\delta}_i[k+2|k]$ can be computed, with acceptable precision and using only information originating from $\mathcal{N}_i$, by sufficiently increasing the sampling rate of the control system.

With this being said, we conclude the presentation of our control laws and we move on to exemplifying their numerous practical benefits, via a series of numerical simulations.

[2]Ultimately, given that we are referring to scalar quantities, the weighting process boils down to the relative ratio of the two values.

IV. Simulations and Numerical Results

A. Parameters of the Control Laws

For the network presented in Section II, we now lay out the parameters which allow for the implementation of the control laws discussed in Section III. We begin with the NRF-based subcontrollers, and we employ the design procedure outlined in Section III-A to obtain control laws of type (4) which satisfy the objectives stated in points *i*)–*iii*) from Section II-C.

We aim to design a control system which ensures rapid closed-loop response, in order to quickly attenuate the propagation of disturbance throughout the network. This goal is especially important, since all of the network's nodes are highly susceptible to $w_5[k]$, in the distributed setting in which we are operating (recall Figure 1). In order to ensure both the stabilization of the grid's dynamics and the rapid rejection of disturbance, we employ *deadbeat control* (see, for example, Section 10.8 of [18]) in the NRF framework, by placing all of the closed-loop system's poles in $z = 0$, while also satisfying the structural constraints imposed by the neighbourhoods given in (3). By doing so, we obtain the distributed and stabilizing control laws from (7), located at the top of the next page.

The second component of our proposed control scheme is far more straightforward to describe, and to design. For the optimization problems given in (5), we choose $u_{\text{lim}} = 0.1$, while also selecting $\beta_{ri} = 10^6$ and $\beta_{ui} = 1$, $\forall\, i \in \{1 : N\}$.

B. Simulation Scenario and Obtained Performance

Suppose we wish to synchronize the electrical angles of all the nodes in our grid according to a reference signal given by

$$r[k] = 0.2 \cdot \mathbb{1}[k-2] - 0.4 \cdot \mathbb{1}[k-52],$$

where $\mathbb{1}[k]$ denotes the discrete-time Heaviside step function. At the same time, we also wish to showcase the ability of our control system to prevent the propagation of disturbance throughout the network. To this end, suppose that the grid's fifth node is subject to the input disturbance signal

$$w_5[k] = 0.075 \cdot (\mathbb{1}[k-100] - \mathbb{1}[k-150]),$$

which, recalling the fact that $\Delta t = 0.2$ s, implies that the fifth node's input will be additively disturbed by a rectangular

$$
\begin{cases}
u_{11}[k] = & 0.0037 \cdot u_{12}[k-2] - 0.0056 \cdot u_{13}[k-2] - 0.0072 \cdot u_{15}[k-2] - 0.00016 \cdot \delta_1[k-2] 0.061 \cdot \delta_2[k-1] \\
& +0.016 \cdot \delta_2[k-2] - 0.012 \cdot \omega_2[k-1] + 0.0064 \cdot \omega_2[k-2] - 0.023 \cdot \delta_3[k-1] - 0.027 \cdot \delta_3[k-2] \\
& -0.0047 \cdot \omega_3[k-1] - 0.011 \cdot \omega_3[k-2] - 0.013 \cdot \delta_5[k-1] - 0.035 \cdot \delta_5[k-2] - 0.0025 \cdot \omega_5[k-1] - 0.014 \cdot \omega_5[k-2], \\
u_{12}[k] = & -0.022 \cdot u_{11}[k-2] + 0.013 \cdot u_{14}[k-2] - 0.019 \cdot u_{15}[k-2] - 0.097 \cdot \delta_1[k-1] - 0.11 \cdot \delta_1[k-2] \\
& -0.019 \cdot \omega_1[k-1] - 0.043 \cdot \omega_1[k-2] + 0.00053 \cdot \delta_2[k-2] - 0.33 \cdot \delta_4[k-1] + 0.055 \cdot \delta_4[k-2] \\
& -0.066 \cdot \omega_4[k-1] + 0.024 \cdot \omega_4[k-2] - 0.11 \cdot \delta_5[k-1] - 0.088 \cdot \delta_5[k-2] - 0.022 \cdot \omega_5[k-1] - 0.036 \cdot \omega_5[k-2], \\
u_{13}[k] = & -0.013 \cdot u_{11}[k-2] + 0.0067 \cdot u_{14}[k-2] - 0.015 \cdot u_{15}[k-2] - 0.032 \cdot \delta_1[k-1] - 0.065 \cdot \delta_1[k-2] \\
& -0.0065 \cdot \omega_1[k-1] - 0.026 \cdot \omega_1[k-2] - 0.00038 \cdot \delta_3[k-2] - 0.14 \cdot \delta_4[k-1] + 0.029 \cdot \delta_4[k-2] \\
& -0.027 \cdot \omega_4[k-1] + 0.013 \cdot \omega_4[k-2] - 0.032 \cdot \delta_5[k-1] - 0.072 \cdot \delta_5[k-2] - 0.0064 \cdot \omega_5[k-1] - 0.029 \cdot \omega_5[k-2], \\
u_{14}[k] = & 0.012 \cdot u_{12}[k-2] - 0.012 \cdot u_{13}[k-2] - 0.024 \cdot u_{15}[k-2] - 0.24 \cdot \delta_2[k-1] + 0.049 \cdot \delta_2[k-2] \\
& -0.047 \cdot \omega_2[k-1] + 0.02 \cdot \omega_2[k-2] - 0.11 \cdot \delta_3[k-1] - 0.059 \cdot \delta_3[k-2] - 0.023 \cdot \omega_3[k-1] - 0.024 \cdot \omega_3[k-2] \\
& +0.00052 \cdot \delta_4[k-2] - 0.057 \cdot \delta_5[k-1] - 0.11 \cdot \delta_5[k-2] - 0.011 \cdot \omega_5[k-1] - 0.047 \cdot \omega_5[k-2], \\
u_{15}[k] = & -0.01 \cdot u_{11}[k-2] - 0.0084 \cdot u_{12}[k-2] - 0.011 \cdot u_{13}[k-2] - 0.011 \cdot u_{14}[k-2] - 0.051 \cdot \delta_1[k-2] \\
& -0.02 \cdot \omega_1[k-2] - 0.039 \cdot \delta_2[k-2] - 0.015 \cdot \omega_2[k-2] - 0.056 \cdot \delta_3[k-2] - 0.022 \cdot \omega_3[k-2] - 0.053 \cdot \delta_4[k-2] \\
& -0.021 \cdot \omega_4[k-2] - 0.0054 \cdot \delta_5[k-2].
\end{cases}
\tag{7}
$$

impulse signal which has non-zero values in the interval $[20\text{ s}, 30\text{ s})$, and whose amplitude is 75% of u_{lim}.

In order to test the properties of our closed-loop system, we initialize each node's electrical angle at random (and with uniform sampling probability) in the interval $[-0.25, 0.25]$, while doing the same for the electrical frequencies, with respect to the interval $[-0.1, 0.1]$. Moreover, we introduce a uniformly distributed additive noise, bounded in amplitude by 10^{-3}, to both the state measurements and to the signals being exchanged between the nodes' subcontrollers. With all this setup now complete, we proceed to implement (7), in which all the delayed signal values are set to zero at time instant $k = 0$, and we solve (5) by using MOSEK [19] via YALMIP [20]. By simulating these control laws in closed-loop configuration with the grid's dynamics, we obtain the results depicted in Figure 2 below. As showcased in the aforementioned figure, the proposed control laws successfully carry out the synchronization of all the electrical angles in the grid, while ensuring adequate transient response properties.

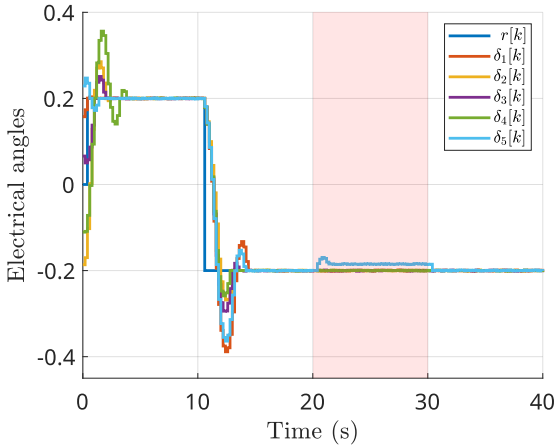

Fig. 2. Tracking performance obtained for the proposed simulation scenario (disturbance-affected interval highlighted via the pink shaded area).

In addition to this, the control scheme manages to contain the effects of $w_5[k]$ to the grid's fifth node, with only $\delta_5[k]$ being noticeably affected by the previously mentioned input disturbance. Given the direct dynamical coupling between the fifth node and all of the other nodes in the considered network, the containment of the desynchronization caused by $w_5[k]$ serves to empirically validate objective $iii)$ from Section II-C.

Finally, we point out that command signals used to ensure the phase synchronization depicted in Figure 2 satisfy the amplitude bounds originating from objective $v)$ in Section II-C. As can be readily seen in Figure 3, which is located at the top of the next page, the absolute values of all the command signals being sent to the grid's nodes are at most $u_{\text{lim}} = 0.1$, throughout the entire runtime of the simulation. Moreover, Figures 4 and 5 (also located on the next page) present detailed views of each layer's computed command signals.

With the effectiveness of our proposed control system now validated upon the grid's dynamics, we proceed to briefly summarize the developments introduced in this paper, and we also address a number of directions for future research.

V. Conclusions and Future Work

The combination between classical MPC-based policies and the distributed control techniques developed in [10] and [11] has been shown to produce promising results for a benchmark synchronization problem, based upon the grid dynamics from [14]. The proposed regulatory strategy accomplishes all of the objectives assigned to it, while also being both straightforward and computationally inexpensive to implement.

The most obvious avenue of improvement is the one related to constraint satisfaction. Indeed, recall that the only *hard constraints* employed in the formulations stated in (5) are those related to the absolute value of each node's command signal, with respect to the current time instant. It goes without saying that the ability to enforce hard constraints on the grid's state variables is a desirable feature in any control system, since these would allow us to place bounds on, for example, the rated electrical frequencies of the nodes or the intensities of

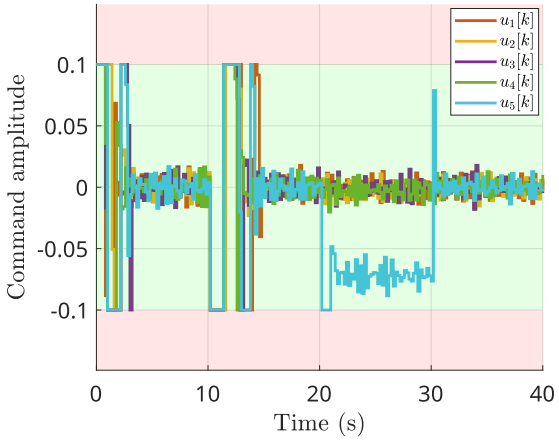

Fig. 3. Command signals associated with the proposed simulation scenario (admissible amplitudes highlighted via the green shaded area).

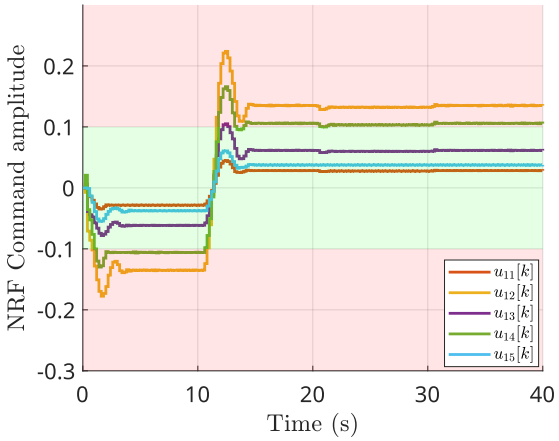

Fig. 4. Command signals associated with the NRF subcontrollers (admissible amplitudes for the signals in Figure 3 highlighted via the green shaded area).

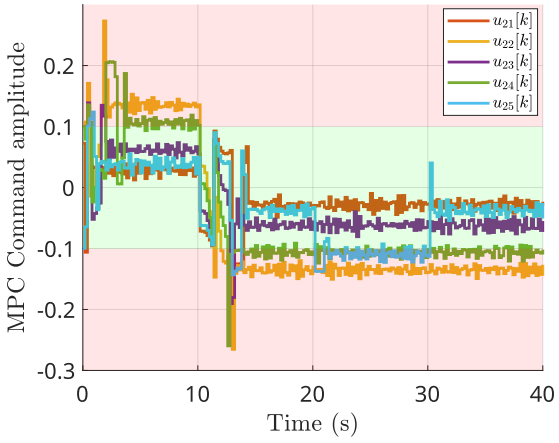

Fig. 5. Command signals associated with the MPC subcontrollers (admissible amplitudes for the signals in Figure 3 highlighted via the green shaded area).

the currents flowing through the grid. Crucially, the availability of constraint-handling mechanisms enables the management of power congestion in the grid [21]. This enticing possibility will form the core of our future research on this topic.

References

[1] B. Meyer, J. Astic, P. Meyer, F. Sardou, C. Poumarede, N. Couturier, M. Fontaine, C. Lemaitre, J. Maeght, and C. Straub, "Power Transmission Technologies and Solutions: The Latest Advances at RTE, the French Transmission System Operator," *IEEE Power and Energy Magazine*, vol. 18, no. 2, pp. 43–52, 2020.

[2] N. Belyaev, Y. Khrushchev, S. Svechkarev, A. Prokhorov, and L. Wang, "Generator to grid adaptive synchronization technique based on reference model," in *Proc. of the 2015 IEEE Eindhoven PowerTech*, pp. 1–5, 2015.

[3] G. Wang, H. Sun, D. Nikovski, and J. Zhang, "A novel BESS-based fast synchronization method for power grids," in *Proc. of the 2017 IEEE Manchester PowerTech*, pp. 1–6, 2017.

[4] T. Nurminen, R. Mourouvin, M. Hinkkanen, J. Kukkola, M. Routimo, A. Vilhunen, and L. Harnefors, "Observer-Based Power-Synchronization Control for Grid-Forming Converters," in *Proc. of the 2023 IEEE Belgrade PowerTech*, pp. 1–6, 2023.

[5] Y.-S. Wang, N. Matni, and J. Doyle, "A System-Level Approach to Controller Synthesis," *IEEE Transactions on Automatic Control*, vol. 64, no. 10, pp. 4079–4093, 2019.

[6] Y.-S. Wang, N. Matni, and J. C. Doyle, "Separable and Localized System-Level Synthesis for Large-Scale Systems," *IEEE Transactions on Automatic Control*, vol. 63, no. 12, pp. 4234–4249, 2018.

[7] C. A. Alonso, J. S. Li, J. Anderson, and N. Matni, "Distributed and Localized Model-Predictive Control–Part I: Synthesis and Implementation," *IEEE Transactions on Control of Network Systems*, vol. 10, no. 2, pp. 1058–1068, 2023.

[8] C. A. Alonso, J. S. Li, N. Matni, and J. Anderson, "Distributed and Localized Model Predictive Control—Part II: Theoretical Guarantees," *IEEE Transactions on Control of Network Systems*, vol. 10, no. 3, pp. 1113–1123, 2023.

[9] Ş. Sabău, C. Oară, S. Warnick, and A. Jadbabaie, "Optimal Distributed Control for Platooning via Sparse Coprime Factorizations," *IEEE Transactions on Automatic Control*, vol. 62, no. 1, pp. 305–320, 2017.

[10] Ş. Sabău, A. Sperilă, C. Oară, and A. Jadbabaie, "Network Realization Functions for Optimal Distributed Control," *IEEE Transactions on Automatic Control*, vol. 68, no. 12, pp. 8059–8066, 2023.

[11] A. Sperilă, C. Oară, B. Ciubotaru, and Ş. Sabău, "Distributed Control of Descriptor Networks: A Convex Procedure for Augmented Sparsity," *IEEE Transactions on Automatic Control*, vol. 68, no. 12, pp. 8067–8074, 2023.

[12] J. Rawlings, D. Mayne, and M. Diehl, *Model Predictive Control: Theory, Computation, and Design, Second Edition*. Nob Hill Publishing, 2020.

[13] F. Borrelli, A. Bemporad, and M. Morari, *Predictive Control for Linear and Hybrid Systems*. Cambridge University Press, 2017.

[14] K. Koorehdavoudi, S. Roy, T. Prevost, F. Xavier, P. Panciatici, and V. Venkatasubramanian, "Input-Output Properties of the Power Grid's Swing Dynamics: Dependence on Network Parameters," in *2019 IEEE Conference on Control Technology and Applications (CCTA)*, pp. 92–97, 2019.

[15] K. Zhou, J. Doyle, and K. Glover, *Robust and Optimal Control*. Prentice-Hall, 1996.

[16] L. Harnefors, M. Rahman, M. Hinkkanen, and M. Routimo, "Reference-Feedforward Power-Synchronization Control," *IEEE Transactions on Power Electronics*, vol. 35, no. 9, pp. 8878–8881, 2020.

[17] C. Kammer and A. Karimi, "Decentralized and Distributed Transient Control for Microgrids," *IEEE Transactions on Control Systems Technology*, vol. 27, no. 1, pp. 311–322, 2019.

[18] B. Kuo, *Digital Control Systems*. Harcourt College Publishers, 1980.

[19] MOSEK ApS, *The MOSEK optimization toolbox for MATLAB manual. Version 10.2*, 2024.

[20] J. Löfberg, "YALMIP : A Toolbox for Modeling and Optimization in MATLAB," *In Proc. of the CACSD Conference*, 2004.

[21] N. Dkhili, S. Olaru, A. Iovine, G. Giraud, J. Maeght, P. Panciatici, and M. Ruiz, "Data-Based Predictive Control for Power Congestion Management in Subtransmission Grids Under Uncertainty," *IEEE Transactions on Control Systems Technology*, vol. 31, no. 5, pp. 2146–2158, 2023.